Helium: Journal of Science and Applied Chemistry
https://helium-fmipa.unpak.ac.id/

Volume 6, Number 1, June 2026, Page 37 - 48
e-ISSN: 2776-4508; p-ISSN: 2776-1711
Publisher : Universitas Pakuan

Comparative Study of Functional Monomers and Crosslinkers in the Synthesis of Molecularly Imprinted Polymers for Selective Removal of Bisphenol A

Lasmaryna Sirumapea [a)], Tri Saputra Tambunan [a)], Maharani Utami [a)], Erjon [a)], Arie Firdiawan [a)], Fitria Puspita[b*)]

[a)] Sekolah Tinggi Ilmu Farmasi Bhakti Pertiwi, *Jl. Ariodillah III No.22A, Palembang, South Sumatra, Indonesia*
[b)] *AKA Bogor Polytechnic, Jl. Pangeran Sogiri No.283, Tanah Baru, Bogor, West Java, Indonesia*
[*)] *Corresponding Author: pipitfpuspita@gmail.com*

DOI: *https://doi.org/10.33751/helium.v6i1.48*
Article history: *received:20-02-2026; revised: 08-05-2026; accepted:12-05-2026; published: 02-06-2026*

ABSTRACT

Bisphenol A (BPA) is an endocrine-disrupting compound associated with documented environmental and health risks. This study evaluates and compares two distinct Molecularly Imprinted Polymer (MIP) architectures synthesized via bulk polymerization for selective BPA adsorption. System A utilized Methacrylic Acid (MAA) crosslinked with Ethylene Glycol Dimethacrylate (EGDMA), while System B employed Acrylamide (AM) with Trimethylolpropane Trimethacrylate (TRIM). FTIR spectroscopy confirmed template-monomer hydrogen bonding, while SEM revealed a porous morphology for System A compared to the dense surface of System B. Batch adsorption results showed that System A achieved a higher maximum capacity (Q_{max} = 14.74 mg/g) and imprinting factor (IF = 7.96) than System B (Q_{max} = 9.1 mg/g; IF = 3.33). These findings are attributed to the hydrogen-bonding affinity of MAA and enhanced site accessibility within the EGDMA matrix. Conversely, System B exhibited a higher selectivity coefficient (α = 4.1) against paracetamol than System A (α = 3.04), reflecting the influence of TRIM-induced rigidity on cavity fidelity. These findings indicate that the AM-TRIM system provides higher selectivity, while the MAA-EGDMA system demonstrates higher adsorption capacity for potential environmental applications.

Keywords: Bisphenol A, MIP, NIP, Selective adsorption

1. Introduction

Bisphenol A (BPA) remains one of the most critical anthropogenic contaminants globally due to its extensive use as a monomer in the production of polycarbonate plastics and epoxy resins. Annual global production capacity has continued to rise, driven by demand for consumer products such as food packaging, thermal paper, and medical devices [1]. However, the ester bonds within these polymeric networks are susceptible to hydrolysis under thermal or chemical stress, leading to the continuous leaching of BPA into food matrices and aquatic ecosystems [2]. As a pervasive endocrine-disrupting chemical (EDC), BPA exhibits strong estrogenic activity by mimicking 17β-estradiol, interfering with hormonal signaling even at trace concentrations (ng/L levels). Epidemiological and toxicological studies have linked chronic BPA exposure to severe health anomalies, including reproductive disorders, metabolic syndrome, and increased susceptibility to hormone-dependent cancers [3,4]. Consequently, regulatory agencies worldwide, including the European Food Safety Authority (EFSA), have progressively lowered the Tolerable Daily Intake (TDI) for BPA, most recently setting a new threshold of 0.2 ng/kg bw/day, necessitating the development of highly sensitive and selective remediation technologies [5].

Conventional methods for BPA detection and quantification, such as High-Performance Liquid Chromatography (HPLC) coupled with Mass Spectrometry (MS), offer high sensitivity but are often constrained by complex sample preparation, high operational costs, and the need for large volumes of organic solvents [6,7]. On the other hand, conventional

Volume 6, Number 1, June 2026, Page 37 - 48
e-ISSN: 2776-4508; p-ISSN: 2776-1711
Publisher : Universitas Pakuan

remediation methods for BPA removal, such as the use of activated carbon in water treatment, often lack selectivity. This results in the competitive adsorption of non-target organic matter and reduced efficiency for specific pollutants like BPA [8-10]. To address these limitations, Molecular Imprinting Technology (MIT) has emerged as a robust strategy for synthesizing materials often referred to as "artificial antibodies" due to their high specificity. Molecularly Imprinted Polymers (MIPs) are synthesized by polymerizing functional monomers and crosslinkers around a template molecule [11, 12]. The subsequent extraction of the template leaves behind three-dimensional cavities complementary in shape, size, and chemical functionality to the target analyte [13-15]. Figure 1 below shows a schematic illustration of MIPs synthesis.

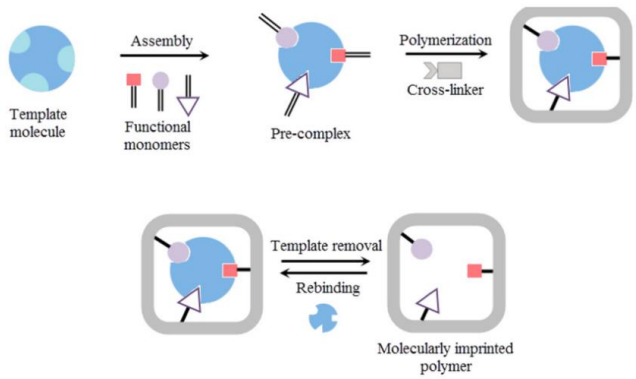

Figure 1. Schematic diagram of molecular imprinting of polymer [16].

The adsorption performance of MIPs is fundamentally governed by the synergistic interaction between the functional monomer and the crosslinker. The selection of the functional monomer dictates the affinity of the recognition sites [12]. Methacrylic acid (MAA) is widely regarded as a "universal monomer" for BPA imprinting due to the ability of its carboxylic groups to form strong hydrogen bonds with the hydroxyl groups of BPA [17-19]. However, neutral monomers like Acrylamide (AM) offer an alternative interaction mechanism, relying on amide functionalities that may provide distinct selectivity patterns in aqueous environments where ionization can affect binding stability [20-22].

Equally critical is the role of the crosslinker, which fixes the functional groups in specific spatial orientations. Bifunctional crosslinkers, such as Ethylene Glycol Dimethacrylate (EGDMA), are commonly employed to create flexible, accessible polymeric networks [23, 24]. In contrast, trifunctional crosslinkers like Trimethylolpropane Trimethacrylate (TRIM) introduce higher crosslinking density and rigidity [25-27]. While theoretical studies suggest that increased rigidity enhances the fidelity of the imprinted cavity, thereby improving selectivity, it often imposes mass transfer resistance that can compromise total adsorption capacity [12-14].

Despite the extensive literature on MIP synthesis for BPA, few studies have conducted a direct, comparative analysis of the trade-offs between capacity and selectivity using these distinct architectural systems. Most research focuses on optimizing a single system rather than elucidating how the interplay between monomer acidity (MAA vs. AM) and crosslinker functionality (EGDMA vs. TRIM) influences the discrimination of BPA from structural analogues. This study compares two MIP architectures for selective BPA adsorption: System A (MAA-EGDMA) and System B (AM-TRIM). Earlier studies have established that methacrylic acid (MAA) and acrylic acid are primarily utilized as functional monomers for non-covalent imprinting due to their straightforward synthesis protocols. Computational analyses have confirmed that MAA is highly compatible with a wide variety of target compounds [28]. Similarly, acrylamide (AM) provides amide groups capable of forming strong hydrogen bonds, which are essential for non-covalent imprinting, particularly in polar or aqueous environments.

Regarding the crosslinkers, EGDMA is universally employed due to its broad template compatibility. However, studies investigating the trifunctional crosslinker TRIM have demonstrated that, compared to EGDMA, TRIM imparts greater structural stiffness and yields more efficient binding cavities. For instance, MIPs utilizing TRIM have been reported to exhibit higher binding and adsorption properties than those using EGDMA [27, 29].

Building on these foundational characteristics, our study deliberately compares these contrasting systems (MAA-EGDMA and AM-TRIM) specifically for the selective adsorption of Bisphenol A. By

Volume 6, Number 1, June 2026, Page 37 - 48
e-ISSN: 2776-4508; p-ISSN: 2776-1711
Publisher : Universitas Pakuan

evaluating their physicochemical and adsorption properties, this research aims to elucidate the fundamental structural trade-off between adsorption capacity, driven by an accessible hydrogen-bonding network, and spatial selectivity, maintained by a rigid matrix. Ultimately, these findings provide a clear guide for tailoring MIP configurations, distinguishing between the requirements for high-capacity environmental remediation and high-precision analytical sensing.

2. Methods

This section details the materials, instrumentation, and experimental protocols used to synthesize and evaluate the BPA-imprinted polymers. Information regarding reagent sources, analytical tools, and standardized procedures for polymerization, template removal, and adsorption studies is provided to ensure the study's reproducibility.

2.1. Materials

The chemicals utilized in this study were categorized into template molecules, functional monomers, crosslinkers, initiators, and solvents. Bisphenol A (BPA, 99%) was selected as the template molecule. Methacrylic Acid (MAA) and Acrylamide (AM, 99%, HPLC grade) were employed as functional monomers. Both the template and monomers were purchased from Sigma-Aldrich (St. Louis, MO, USA). The crosslinking agents, Ethylene Glycol Dimethacrylate (EGDMA) and Trimethylolpropane Trimethacrylate (TRIM), as well as the radical initiator Benzoyl Peroxide (BPO, Luperox® A70S), were also supplied by Sigma-Aldrich. The porogenic solvent, Acetonitrile (HPLC grade), was obtained from Merck (Darmstadt, Germany). Solvents for extraction and washing included Methanol (HPLC grade, Sigma-Aldrich) and Glacial Acetic Acid (Analytical Reagent grade, PT. Smart-Lab Indonesia). Double-distilled water was used throughout the experimental procedures. All chemicals were used as received without further purification.

2.2. Instrumentation

The chemical functional groups of the synthesized polymers were analyzed using a Shimadzu Fourier Transform Infrared (FTIR) spectrophotometer (Japan). Surface morphology and porosity were examined using a JEOL JSM-6510 LA Scanning Electron Microscope (SEM, Japan). Quantitative analysis of BPA concentration was performed using UV-Vis Spectrophotometers (Shimadzu and Thermo Scientific™ GENESYS™ 150). Absorbance measurements were conducted at the maximum wavelength (λ_{max}) of 276 nm. Batch adsorption experiments were carried out using a DLAB orbital shaker, and mass measurements were performed using a Fulgid/Quattro analytical balance.

2.3. Synthesis of Molecularly Imprinted Polymers (MIPs)

Two distinct MIP architectures (System A and System B) were synthesized via bulk polymerization. The formulations were designed to compare the performance of acidic versus neutral monomers with different crosslinker functionalities. These formulations were all in mole base. A previous study reported the composition of the template: functional monomer: crosslinker was about 1 : (4–6) : (10–20) [30].

- **System A (MAA-co-EGDMA):** This system followed the acidic monomer pathway. BPA (0.228 g) was dissolved in 10 mL of acetonitrile. Methacrylic Acid (MAA, 0.337 mL) was added as the functional monomer, followed by EGDMA (3.96 mL) as the crosslinker and BPO (125 mg) as the initiator
- **System B (AM-co-TRIM):** This system followed the neutral monomer pathway. BPA (0.288 g) was dissolved in 20 mL of acetonitrile. Acrylamide (AM, 0.35 g) was added as the functional monomer, along with the trifunctional crosslinker TRIM (6.37 mL) and BPO (100 mg).

The prepolymerization mixtures were sonicated to ensure homogeneity and purged with nitrogen gas to remove dissolved oxygen. Polymerization was conducted in a temperature-controlled oven at 70 °C. The reaction time was set to 3 hours for System A and 5 hours for System B to accommodate the steric hindrance of the trifunctional crosslinker [31, 32]. The resulting rigid monoliths were

Volume 6, Number 1, June 2026, Page 37 - 48
e-ISSN: 2776-4508; p-ISSN: 2776-1711
Publisher : Universitas Pakuan

crushed, ground, and sieved to obtain particles passing through a 20-mesh sieve. This size was selected based on established protocols to provide an optimal balance between ensuring adequate surface area for effective adsorption and facilitating efficient solid-liquid separation during the batch experiments. Non-imprinted polymers (NIPs) were prepared simultaneously under identical conditions but without the addition of the BPA template.

2.4. Template Removal

The removal of the BPA template was achieved through solvent extraction, with methods tailored to the polymer rigidity.

- **System A**: A batch extraction method was employed using a mixture of methanol and acetic acid (8.5:1.5 v/v). The polymer particles were agitated for 24 hours to ensure complete template removal.
- **System B**: A Soxhlet extraction technique was utilized with a mixture of methanol and acetic acid (9:1 v/v) at 80 °C for 24 hours to facilitate deep-pore cleaning.

The extraction process was monitored by UV-Vis spectroscopy until no BPA was detected in the supernatant. Finally, the polymers were washed with methanol to remove residual acid and dried at 60 °C.

2.5. Characterization

The physicochemical properties of the synthesized polymers were characterized to confirm the successful imprinting process and to evaluate morphological differences.

2.5.1. Fourier Transform Infrared (FTIR) Spectroscopy

Functional group analysis was performed to verify the incorporation of monomers and the presence of specific interactions within the polymer matrix. The samples were prepared using the standard potassium bromide (KBr) pellet technique. Approximately 2 mg of polymer powder was mixed with 200 mg of spectroscopic-grade KBr and pressed into a transparent pellet. The spectra were recorded in the wavenumber range of 4000–500 cm^{-1}.

2.5.2. Scanning Electron Microscopy (SEM)

The surface morphology and porosity of the polymer particles were examined using SEM. Before analysis, the non-conductive polymer samples were mounted on aluminum stubs using double-sided carbon tape and subjected to gold sputter coating to enhance electron conductivity and prevent surface charging. The surface structure was observed at a magnification of 40,000x using an accelerating voltage of 15 kV, a working distance of 1 mm, and a Secondary Electron Imaging (SEI) detector mode to visualize the bulk structure and pore distribution.

2.6. Adsorption and Selectivity Studies

All batch adsorption experiments were performed in triplicate to ensure the reliability and reproducibility of the data, with the results reported as mean ± standard deviation. The equilibrium adsorption capacity (Q) was determined by calculating the difference between the initial and equilibrium BPA concentrations, normalized to the polymer mass and solution volume, and determined following equation 1.

$$Q = \frac{(C_0 - C_t)}{m} V \quad (1)$$

where Q = adsorption capacity (mg/g), C_0 = analyte concentration before adsorption (50 mg/L), Ct = analyte concentration after adsorption (mg/L), m = mass of sorbent (mg), and V = solution volume (mL).

Furthermore, the imprinting efficiency and selectivity were evaluated using the Imprinting Factor (IF) and Selectivity Coefficient (α), which represent the ratio of adsorption capacities between the MIP/NIP and the target/analogue molecules, respectively, and calculated according to equation 2.

$$IF = \frac{\text{Q of polymer with analyte after extraction}}{\text{Q of polymer built without analyte}} \quad (2)$$

Considering the other molecules were also observed to evaluate the selectivity, called selectivity coefficient (α)-paracetamol was chosen in this evaluation; then α determined according to equation 3.

$$\alpha = \frac{\text{Q BPA}}{\text{Q analogue molecule}} \quad (3)$$

Volume 6, Number 1, June 2026, Page 37 - 48
e-ISSN: 2776-4508; p-ISSN: 2776-1711
Publisher : Universitas Pakuan

3. Results and Discussion

3.1. Physicochemical Characterization

The detailed physicochemical properties of the synthesized polymers were investigated to confirm the successful formation of imprinted cavities and to elucidate the structural differences resulting from the variations in monomer acidity and crosslinker functionality. Specifically, spectroscopic analysis was employed to verify the chemical interactions between the template and the polymer matrix, while microscopic analysis was conducted to assess the surface topography and porosity, which are critical determinants of adsorption performance.

The structural integrity and functional group composition of the synthesized MIPs and NIPs for both systems were systematically verified through comparative FTIR spectroscopy. The success of the polymerization process and the presence of characteristic functional groups were evaluated by comparing the infrared absorption profiles, as presented in Figure 2.

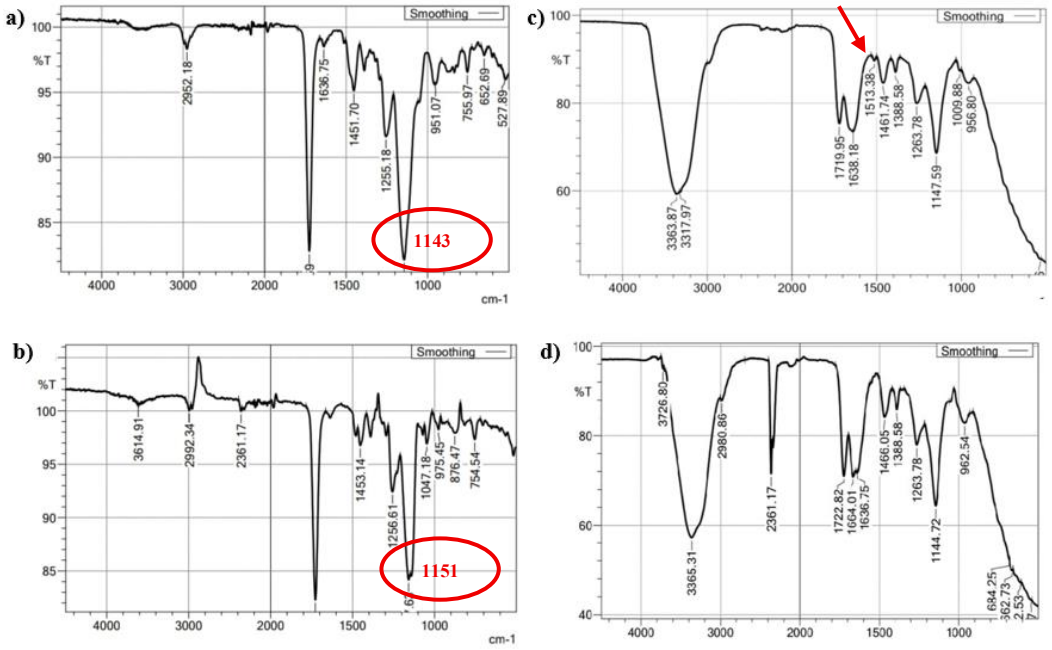

Figure 2. FTIR Spectra of MIP and NIP of (a) MIP System A (MAA-EGDMA), (b) NIP System A, (c) MIP System B (AM-TRIM), and (d) NIP System B.

A fundamental indicator of successful free-radical polymerization in both systems is the complete disappearance of the vinyl C=C stretching vibration at 1637 cm^{-1} and the =C-H out-of-plane bending at 950 cm^{-1} [34]. In all spectra (a–d), the absence of these sharp monomeric peaks confirms that the BPO-initiated reaction effectively converted unsaturated precursors into a saturated aliphatic backbone, further corroborated by sp^3 hybridized C-H stretching vibrations observed in the 2850–3000 cm^{-1} region.

For System A (MAA-co-EGDMA), the chemical identity is dominated by the ester and carboxylic functionalities. The spectra (a and b) exhibit an intense, sharp peak at 1730 cm^{-1}, representing the C=O stretching of EGDMA ester groups overlapping with the carboxylic C=O of MAA. Molecular recognition in this system is driven by hydrogen bonding between the phenolic hydroxyls of BPA and the carboxylic sites of MAA. This interaction is evidenced by the O-H absorption band at 3450 cm^{-1}, which appears broader and more intense in the MIP spectrum compared to the NIP, indicating a high density of hydrogen-bonded complexes [35].

In addition, for system A, both polyers have similar functional groups; no significant difference was shown in the MIP and NIP spectra of Infra red spectrum due to the constituents of the compound. The main difference that can be observed is the shift of the wave

Volume 6, Number 1, June 2026, Page 37 - 48
e-ISSN: 2776-4508; p-ISSN: 2776-1711
Publisher : Universitas Pakuan

number of NIP and MIP. In system A, in the MIP spectrum, the C-O-C functional group derived from methyl methacrylic acid was found at a wave number of 1143 cm^{-1}, while in NIP, the presence of the C-O-C functional group was detected at a wave number of 1151 cm^{-1}. This wave number shift is caused by the interaction between the template molecules contained in MIP and the functional monomer; in NIP, this interaction does not occur because there is no bisphenol A, template molecule, applied.

In contrast, System B (AM-co-TRIM) presents a distinct profile characterized by acrylamide units. The NIP spectrum (d) shows primary amide markers through the Amide I band (C=O stretch) at 1682 cm^{-1} and the Amide II band (N-H bending) at 1610 cm^{-1}. Notably, a significant "red shift" of the Amide I peak from 1682 cm^{-1} in the NIP to 1675 cm^{-1} in the MIP (c) confirms that the amide group acts as a proton acceptor for BPA, forming a stable imprinted complex [18]. The dense ester linkages from the trifunctional TRIM crosslinker are also visible at 1735 cm^{-1}, providing the requisite rigidity for cavity shape fidelity [27].

A small peak found at wave number 1513 cm^{-1} represented the C=C. This peak was not visible in NPBM; this is likely due to the addition of a C=C group to PBM from Bisphenol-A.

The success of the template removal process was verified by the disappearance of the characteristic BPA aromatic ring vibrations at 1510 cm^{-1} in the MIP spectra. Following extraction, the carbonyl and amide peaks in the MIPs exhibited "spectral recovery," shifting back toward the original NIP frequencies. This phenomenon confirms that the functional sites have been effectively liberated, leaving behind specific recognition cavities ready for selective BPA rebinding in analytical applications.

3.2. Morphological Characterization

The surface morphology and structural topography of the synthesized MIPs and NIPs were evaluated via Scanning Electron Microscopy (SEM) to correlate the internal molecular imprinting with the external physical characteristics of the polymer matrices. The representative micrographs illustrating the morphological variations between the imprinted and non-imprinted materials for both systems are presented in Figure 3.

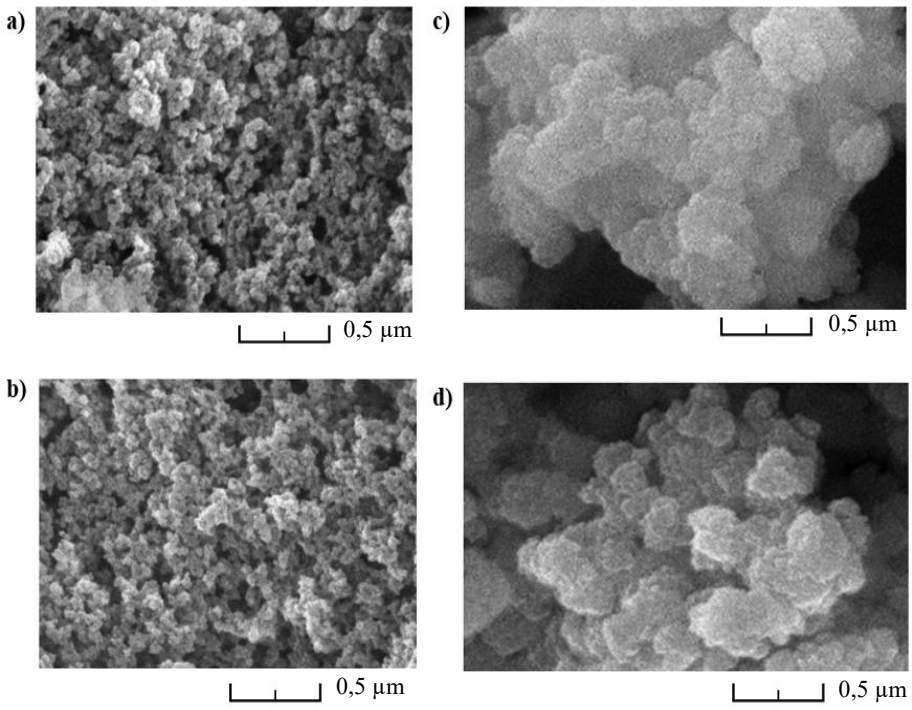

Figure 3. Scanning Electron Microscopy (SEM) micrographs of (a) MIP System A (MAA-EGDMA), (b) NIP System A, (c) MIP System B (AM-TRIM), and (d) NIP System B. All images were recorded at a magnification of 40,000×.

Volume 6, Number 1, June 2026, Page 37 - 48
e-ISSN: 2776-4508; p-ISSN: 2776-1711
Publisher : Universitas Pakuan

For System A (MAA-co-EGDMA), the NIP (Figure 3b) exhibits a relatively smooth, compact, and continuous surface, which is characteristic of polymers synthesized in the absence of a template molecule [17]. In contrast, the MIP System A (Figure 3a) displays a significantly rougher and more fragmented morphology, consisting of submicron spherical aggregates. This increase in surface roughness and the presence of visible micro-voids are indicative of the successful formation of specific recognition cavities and the subsequent extraction of the BPA template [33, 34]. The use of acetonitrile as a porogen in System A facilitates the development of a mesoporous structure, which is essential for enhancing the mass transfer kinetics during BPA rebinding [35].

In System B (AM-co-TRIM), the morphological differences are even more pronounced due to the trifunctional nature of the TRIM cross-linker. The NIP System B (Figure 3d) shows a dense and highly integrated polymer network. However, the MIP System B (Figure 3c) reveals a "cauliflower-like" conglomerate structure with a high degree of porosity. Recent studies [27, 36] suggest that TRIM-based MIPs typically exhibit a higher specific surface area and more rigid structural integrity compared to EGDMA-based systems. The higher cross-linking density of TRIM preserves the three-dimensional architecture of the binding sites, preventing cavity collapse after template removal. This result is consistent with the FTIR data, where the robust ester framework of TRIM supports a more defined porous network, providing better accessibility for BPA molecules to reach the functional amide sites [37].

The SEM analysis confirms that the inclusion of the BPA template during the polymerization process significantly disrupts the polymer packing, leading to a more porous and heterogeneous surface in the MIPs compared to the NIPs. This morphological differentiation is a prerequisite for high-performance molecularly imprinted materials, as the porous structure provides the necessary pathways for rapid diffusion and selective adsorption in analytical applications [36].

3.3. Evaluation of Adsorption Capacity

The equilibrium adsorption performance of the synthesized polymers was evaluated to determine the maximum adsorption capacity (Q_{max}) under saturation conditions and room temperature. The comparative results demonstrate a significant disparity in adsorption capability between the two distinct MIP architectures, driven by the interplay between monomer affinity and crosslinker rigidity. System A (MAA-co-EGDMA) exhibited a significantly higher adsorption capacity, with a Q_{max} value of 14.74 mg/g. This superior performance is attributed to two synergistic factors. Chemically, the carboxylic acid groups of Methacrylic Acid (MAA) serve as potent hydrogen bond donors. As established in fundamental imprinting studies, acidic monomers like MAA form more stable and robust hydrogen bonds with the phenolic hydroxyl groups of BPA in aprotic solvents compared to neutral monomers [33, 34, 38]. Structurally, the bifunctional crosslinker EGDMA creates a relatively more accessible polymeric network. This architecture minimizes mass transfer resistance, allowing the bulky BPA molecules to diffuse more effectively into binding sites located within the polymer matrix [14].

In contrast, System B (AM-co-TRIM) achieved a lower capacity of 9.10 mg/g. While the amide groups of Acrylamide can interact with BPA via hydrogen bonding, the limiting factor in this system is the crosslinker architecture. The trifunctional nature of TRIM imposes a high crosslinking density, resulting in a significantly more rigid and compact matrix [12]. This compactness creates steric hindrance that restricts the accessibility of the deeply embedded imprinted cavities. Consequently, adsorption in System B is likely confined to surface-accessible sites, preventing the full utilization of the internal binding capacity [27]. These findings highlight a fundamental "capacity-selectivity trade-off," where increased rigidity enhances cavity fidelity but simultaneously imposes diffusion limitations that compromise total uptake.

3.4. Selectivity and Molecular Recognition: The Performance Trade-off

To evaluate the specific recognition capability of the imprinted cavities, competitive adsorption studies were conducted using Paracetamol as a

Volume 6, Number 1, June 2026, Page 37 - 48
e-ISSN: 2776-4508; p-ISSN: 2776-1711
Publisher : Universitas Pakuan

structural analogue. Paracetamol was selected due to its structural similarity to BPA (presence of a phenolic moiety) but distinct spatial geometry. The experimental data, as detailed in Table 1, highlight a fundamental trade-off between adsorption capacity and selectivity, a phenomenon widely documented in molecular imprinting technology [12,14]. In line with general MIP practice, the selectivity coefficient (α) was defined as the ratio of distribution coefficients (or adsorbed amounts) of BPA to the analogue at identical concentrations, such that a higher α reflects stronger preferential binding [39, 40]. Values close to unity indicate poor discrimination, whereas values above ~3–4 are typically associated with pronounced molecular recognition [41, 42].

Table 1. Comparative adsorption performance and selectivity parameters (n=3)

Parameter	System A ± SD	System B ± SD
Adsorption Capacity (Q, mg/g)	14.74 ± 0.47	9.10 ± 0.35
Imprinting Factor (IF)	7.96 ± 0.33	3.33 ± 0.10
Selectivity Coefficient (α)	3.04 ± 0.11	4.10 ± 0.13

Although System A demonstrated a superior Imprinting Factor (IF = 7.96 ± 0.33), indicating a high density of generated sites, it exhibited a lower selectivity coefficient against Paracetamol (α = 3.04 ± 0.11). This suggests that the flexibility of the EGDMA-based backbone allows for a degree of polymer swelling or conformational adaptation in aqueous environments. While this flexibility facilitates mass transfer and boosts total capacity, it compromises the "lock-and-key" precision, permitting the non-specific binding of structural analogues that do not perfectly match the template's shape [43].

Conversely, System B demonstrated higher molecular recognition specificity, achieving the highest selectivity coefficient of α = 4.10 ± 0.13. This increased discrimination is the defining advantage of the TRIM-based architecture. The structural rigidity provided by the trifunctional crosslinker effectively "freezes" the polymer network, preserving the fidelity of the cavity shape with high precision [14,27]. This rigid framework prevents the cavity from deforming to accommodate the Paracetamol molecule, thereby effectively excluding the analogue despite its chemical similarity. These findings suggest that while the MAA-EGDMA system is preferable for high-capacity removal, the AM-TRIM system offers the requisite specificity for analytical sensing applications.

4. Conclusion

This study successfully demonstrated the synthesis and comparative evaluation of two distinct Molecularly Imprinted Polymer (MIP) architectures for the selective adsorption of Bisphenol A (BPA). The results confirm that the chemical nature of the functional monomer and the structural rigidity of the crosslinker fundamentally dictate the polymer's performance. The MAA-EGDMA system (System A) proved to be the superior adsorbent in terms of capacity and imprinting efficiency, achieving a maximum adsorption capacity of 14.74 mg/g and an imprinting factor of 7.96. This performance is attributed to the strong hydrogen-bonding affinity of methacrylic acid and the enhanced site accessibility within the EGDMA-based matrix. In contrast, the AM-TRIM system (System B) provided enhanced structural fidelity, resulting in a higher selectivity coefficient (α = 4.1) against the structural analogue paracetamol. These findings underscore a critical performance trade-off: while bifunctional crosslinkers like EGDMA facilitate better mass transfer and total uptake, making them ideal for large-scale environmental sequestration, trifunctional crosslinkers like TRIM enhance cavity rigidity and molecular recognition, making them more suitable for high-precision analytical sensing. Overall, this research provides a strategic framework for tailoring MIP architectures based on the specific requirements of the intended application, whether prioritizing total remediation capacity or high-fidelity molecular detection.

CRediT Authorship Contribution Statement

LS: Conceptualization, Methodology, Supervision, Resources. TST: Investigation, Data Curation, Formal Analysis. MU: Investigation, Data Curation, Formal Analysis. AF: Supervision, Validation, Writing – Review & Editing. ER: Supervision, Validation, Writing – Review & Editing. FP: Writing – Original

Volume 6, Number 1, June 2026, Page 37 - 48
e-ISSN: 2776-4508; p-ISSN: 2776-1711
Publisher : Universitas Pakuan

Draft, Writing – Review & Editing, Project Administration.

Declaration of Competing Interest

The authors declare that they have no known competing financial interests or personal relationships that could have appeared to influence the work reported in this paper.

Data Availability

All data generated or analyzed during this study are included in this published article.

Acknowledgment

The authors did not receive any specific grant from funding agencies in the public, commercial, or not-for-profit sectors.

References

[1] A. Abraham and P. Chakraborty, "A review on sources and health impacts of bisphenol A", *Reviews on Environmental Health*, vol. 35, no. 2, pp. 201–210, Nov. 2020. https://doi.org/10.1515/reveh-2019-0034

[2] O. E. Ohore and S. Zhang, "Endocrine disrupting effects of bisphenol A exposure and recent advances on its removal by water treatment systems. A review", *Scientific African*, vol. 5, p. e00135, Sept. 2019. https://doi.org/10.1016/j.sciaf.2019.e00135

[3] Y. Ma, H. Liu, J. Wu, L. Yuan, Y. Wang, X. Du, ... and H. Wang, "The adverse health effects of bisphenol A and related toxicity mechanisms", *Environmental Research*, vol. 176, 108575, Sept. 2019. https://doi.org/10.1016/j.envres.2019.108575

[4] I. Cimmino, F. Fiory, G. Perruolo, C. Miele, and F. Beguinot, "Potential mechanisms of bisphenol A (BPA) contributing to human disease", *International Journal of Molecular Sciences*, vol. 21, no. 16, pp. 5761, Aug. 2020. https://doi.org/10.3390/ijms21165761

[5] C. Lambré, J. M. Barat Baviera, L. Bolognini, A. Chesson, P. S. Cocconcelli, ... and I. L. Steffensen, "Re-evaluation of the risks to public health related to the presence of bisphenol A (BPA) in foodstuffs", *EFSA Journal*, vol. 21, no. 4, e06857, Apr. 2023. https://doi.org/10.2903/j.efsa.2023.6857

[6] A. Kubiak and M. Biesaga, "Application of molecularly imprinted polymers for bisphenols extraction from food samples–A review", *Critical reviews in analytical chemistry*, vol. 50, no. 4, pp. 311-321, June 2019. https://doi.org/10.1080/10408347.2019.1626698

[7] C. E. Pop, B. A. Miu, D. Németh, R. Wolff, D. F. Mihăilescu, S. M. Avramescu, and M. Mernea, "Bisphenol A analysis and quantification inconsistencies via HPLC-UV: a systematic review with technical notes", *Discover Applied Sciences*, vol. 6, no. 4, 171, Mar. 2024. https://doi.org/10.1007/s42452-023-05617-z

[8] S. Satyam and S. Patra, "Innovations and challenges in adsorption-based wastewater remediation: A comprehensive review," *Heliyon*, vol. 10, no. 9, p. e30206, May 2024 https://doi.org/10.1016/j.heliyon.2024.e29573

[9] F. Cheng and J. Wang, "Removal of bisphenol a from wastewater by adsorption and membrane separation: Performances and mechanisms", *Chemical Engineering Journal*, vol. 484, no. 15, 149414, Mar. 2024. https://doi.org/10.1016/j.cej.2024.149414

[10] Y. Xu, Y. Wu, B. Bhargawa, S. H. Hong, and I. K. Yoo, "The selective removal of bisphenol A using a magnetic adsorbent fused with bisphenol A-binding peptides", *Materials*, vol. 17, no. 7, 1651, Apr. 2024. https://doi.org/10.3390/ma17071651

[11] K. Haupt, A. V. Linares, M. Bompart, and B. T. S. Bui, "Molecularly Imprinted Polymers", *In: Haupt, K. (eds) Molecular Imprinting.*

Volume 6, Number 1, June 2026, Page 37 - 48
e-ISSN: 2776-4508; p-ISSN: 2776-1711
Publisher : Universitas Pakuan

Topics in Current Chemistry, vol. 325. Springer, Berlin, Heidelberg, Dec. 2011. https://doi.org/10.1007/128_2011_307

[12] L. Chen, X. Wang, W. Lu, X. Wu, and J. Li, "Recent advances in molecular imprinting technology: current status, challenges and highlighted applications", *Chemical Society Reviews*, vol. 45, no. 8, pp. 2137–2211, Mar. 2016. https://doi.org/10.1039/C6CS00061D

[13] G. Vasapollo, R. D. Sole, L. Mergola, M. R. Lazzoi, A. Scardino, S. Scorrano, and G. Mele,, "Molecularly imprinted polymers: present and future prospective", *International Journal of Molecular Sciences*, vol. 12, no. 9, pp. 5908-5945, Sept. 2011. https://doi.org/10.3390/ijms12095908

[14] J. J. BelBruno, "Molecularly imprinted polymers", *Chemical reviews*, vol. 119, no.1, pp. 94-119, Sept. 2018. https://doi.org/10.1021/acs.chemrev.8b00171

[15] M. Garg and N. Pamme, "Strategies to remove templates from molecularly imprinted polymer (MIP) for biosensors", *TrAC Trends in Analytical Chemistry*, vol. 170, 117437, Jan. 2024. https://doi.org/10.1016/j.trac.2023.117437

[16] S. Ostrovidov, M. Ramalingam, H. Bae, G. Orive, T. Fujie, T. Hori, ... and H. Kaji,, "Molecularly imprinted polymer-based sensors for the detection of skeletal-and cardiac-muscle-related analytes", Sensors, vol. 23, no. 12, p. 5625, June 2023. https://doi.org/10.3390/s23125625

[17] X. Shi, A. Wu, Q. Qu, R. Li, and D. Zhang, "Development and characterisation of molecularly imprinted polymers based on methacrylic acid for selective recognition of drugs", *Biomaterials*, vol. 28, no. 25, pp. 3741-3749, Sept. 2007. https://doi.org/10.1016/j.biomaterials.2007.04.036

[18] K. Golker, G. D. Olsson, and I. A. Nicholls, ,"The influence of a methyl substituent on molecularly imprinted polymer morphology and recognition–Acrylic acid versus methacrylic acid", *European Polymer Journal*, vol. 92, pp. 137-149, July 2017. https://doi.org/10.1016/j.eurpolymj.2017.04.043

[19] K. Nishchaya, V. K. Rai, and H. Bansode, "Methacrylic acid as a potential monomer for molecular imprinting: a review of recent advances", *Results in Materials*, vol. 18, 100379, June 2023. https://doi.org/10.1016/j.rinma.2023.100379

[20] T. Kanai, Sanskriti C., P. Vislawath, and A. B. Samui, "Acrylamide based molecularly imprinted polymer for detection of m-nitrophenol", *Journal of Nanoscience and Nanotechnology*, vol. 13, no. 4, pp. 3054-3061, Apr. 2013. https://doi.org/10.1166/jnn.2013.7399

[21] M. Boukadida, N. Jaoued-Grayaa, A. Anene, Y. Chevalier, and S. Hbaieb, "Effect of cross-linking agents on the adsorption of histamine on molecularly imprinted polyacrylamide", *Polymer*, vol. 268, 125724, Feb. 2023. https://doi.org/10.1016/j.polymer.2023.125724

[22] A. Poliwoda, M. Mościpan, and P. P. Wieczorek, "Application of molecular imprinted polymers for selective solid phase extraction of bisphenol A", *Ecological Chemistry and Engineering S*, vol. 23, no. 4, pp. 651-664, Dec. 2016. https://doi.org/10.1515/eces-2016-0046

[23] M. Sibrian-Vazquez and D. A. Spivak, "Improving the strategy and performance of molecularly imprinted polymers using cross-linking functional monomers", *The Journal of Organic Chemistry*, vol. 68, no. 25, pp. 9604-9611, Nov. 2023. https://doi.org/10.1021/jo0352225

[24] R. Suravajhala, H. R. Burri, and B. Malik, "Development of highly specific and selectively recognizing caffeine imprinted

Volume 6, Number 1, June 2026, Page 37 - 48
e-ISSN: 2776-4508; p-ISSN: 2776-1711
Publisher : Universitas Pakuan

polymer nanomaterials with EGDMA crosslinker", *Current Nanomaterials*, vol. 6, no. 1, pp. 65-72, June 2021. https://doi.org/10.2174/24054615066662h10603121936

[25] I. Susanti, N. I. S. A. Safitri, R. Pratiwi, and A. N. Hasanah, "Synthesis of molecular imprinted polymer salbutamol using methacrylic acid monomer and trimethyl propane trimethacrylate (trim) as a cross-linker through suspension polymerization", *Int. J. Appl. Pharm*, vol. 14, pp. 32-39, Dec. 2022. https://doi.org/10.22159/ijap.2022.v14s5.01

[26] S. Suryana, M. Mutakin, Y. Rosandi, and A. N. Hasanah, "Rational design of salmeterol xinafoate imprinted polymer through computational method: Functional monomer and crosslinker selection", *Polymers for Advanced Technologies*, vol. 33, no. 1, pp. 221-234, Sept. 2021. https://doi.org/10.1002/pat.5507

[27] M. Cegłowski, J. Kurczewska, A. Lusina, T. Nazim, and P. Ruszkowski, "EGDMA-and TRIM-based microparticles imprinted with 5-fluorouracil for prolonged drug delivery", *Polymers*, vol. 14, no. 5, 1027, Mar. 2022. https://doi.org/10.3390/polym14051027

[28] K. Nishchaya, V. K. Rai, and H. Bansode,, "Methacrylic acid as a potential monomer for molecular imprinting: a review of recent advances", *Results in Materials*, vol. 18, p. 100379, June. 2023. https://doi.org/10.1016/j.rinma.2023.100379

[29] T. Pengkamta, M. Mala, C. Klakasikit, P. Kanawuttikorn, P. Boonkorn, A. Chuaejedton, and W. Karuehanon,, "Synthesis and Evaluation of Molecularly Imprinted Polymer as a Selective Material for Vanillin", *Suan Sunandha Science and Technology Journal*, vol. 7, no. 1, pp. 1-6, Jan. 2020. https://doi.org/10.14456/ssstj.2020.2

[30] S. Amin, S. Damayanti, and S. Ibrahim,, "Interaction Study, Synthesis and Characterization of Molecular Imprinted Polymer Using Functional Monomer Methacrylate Acid and Dimethylamylamine as Template Molecule", *Jurnal Ilmu Kefarmasian Indonesia*, vol. 16, no. 1, pp. 12-19, Apr. 2018. https://doi.org/10.35814/jifi.v16i1.430

[31] L. Sirumapea, M. A. Zulfikar, M. B. Amran, and A. Alni,, "Selective solid-phase extraction of meropenem from human blood plasma using a molecularly imprinted polymer", *Indonesian Journal of Chemistry*, vol. 21, no. 5, pp. 1167-1179, Aug. 2021. https://doi.org/10.22146/ijc.64025

[32] N. Zakia, M. A. Zulfikar, and M. B. Amran,, "Synthesis and characterization of α-mangostin imprinted polymers and its application for solid phase extraction", *Advances in materials research*, vol. 9, no. 4, pp. 251-263, Dec. 2020. https://doi.org/10.12989/amr.2020.9.4.251

[33] R. Ardekani, S. Borhani, and B. Rezaei, "Selective molecularly imprinted polymer nanofiber sorbent for the extraction of bisphenol A in a water sample", *Polymer International*, vol. 69, no. 9, pp. 780-793, Sept. 2020. https://doi.org/10.1002/pi.6013

[34] M. Luna Quinto, S. Khan, J. Vega-Chacón, B. Mortari, A. Wong, M. D. P. Taboada Sotomayor, and G. Picasso, "Development and characterization of a molecularly imprinted polymer for the selective removal of brilliant green textile dye from river and textile industry effluents", *Polymers*, vol. 15, no.18, p. 3709, Sept. 2023. https://doi.org/10.3390/polym15183709

[35] M. Hu, Y. Zhang, J. Yang, X. Zhou, Z. Wei, and D. Ding, "Rapid fabrication of molecularly imprinted polymer fibers for solid phase microextraction of bisphenol A", *Se pu= Chinese Journal of*

Volume 6, Number 1, June 2026, Page 37 - 48
e-ISSN: 2776-4508; p-ISSN: 2776-1711
Publisher : Universitas Pakuan

Chromatography, vol. 33, no. 2, pp. 123-131, Feb. 2015. https://doi.org/10.3724/sp.j.1123.2014.10008

[36] M. Sadia, I. Ahmad, Z. Ul-Saleheen, M. Zubair, M. Zahoor, R. Ullah, ... and I. Zekker, "Synthesis and characterization of MIPs for selective removal of textile dye acid black-234 from wastewater sample", *Molecules*, vol. 28, no. 4, 1555, Feb. 2023. https://doi.org/10.3390/molecules28041555

[37] E. Savigni, E. Girometti, L. Sisti, F. Benstoem, D. Pinelli, and D. Frascari, "Development and validation of molecularly imprinted polymers with bio-based monomers to adsorb carbamazepine from wastewater", *Molecules*, vol. 30, no. 12, p. 2533, June 2025. https://doi.org/10.3390/molecules30122533

[38] S. Fauziah, N. H. Soekamto, P. Taba, and M. B. Amran, "Selectivity of β-Sitosterol imprinted polymers as adsorbent", *Journal of Physics: Conference Series*, vol. 979, no. 1, p. 012059, Mar. 2018. https://doi.org/10.1088/1742-6596/979/1/012059

[39] G. Becskereki, G. Horvai, and B. Tóth,, "The selectivity of molecularly imprinted polymers", *Polymers*, vol. 13, no. 11, p. 1781, May. 2021. https://doi.org/10.3390/polym13111781

[40] E. N. Ndunda,, "Molecularly imprinted polymers—A closer look at the control polymer used in determining the imprinting effect: A mini review", *Journal of Molecular Recognition*, vol. 33, no. 11, p. e2855, June. 2020. https://doi.org/10.1002/jmr.2855

[41] D. A. Spivak, R. Simon, and J. Campbell,, "Evidence for shape selectivity in non-covalently imprinted polymers", *Analytica chimica acta*, vol. 504, no. 1, pp. 23-30, Feb. 2004. https://doi.org/10.1016/S0003-2670(03)00946-2

[42] Chin, K. Z., & Chang, S. M. (2025). Insights into the Imprinting and Rebinding Performance of Molecularly Imprinted Hybrids for Bisphenol A and Bisphenol F. *ACS Applied Materials & Interfaces*, *17*(19), 28568-28584. https://doi.org/10.1021/acsami.5c03038

[43] K. Haupt, P. X. Medina Rangel, and B. T. S. Bui, "Molecularly imprinted polymers: antibody mimics for bioimaging and therapy", *Chemical reviews*, vol. 120, no. 17, pp. 9554-9582, July 2020. https://doi.org/10.1021/acs.chemrev.0c00428